

The total density profile of DM halos fitted from strong lensing

Lin Wang^{1,2*}, Da-Ming Chen^{1,2}, Ran Li¹

¹*National Astronomical Observatories, Chinese Academy of Sciences, 20A Datun Road, Chaoyang District, Beijing 100012, China;*

²*School of Astronomy and Space Science, University of Chinese Academy of Sciences, Beijing 100049, China*

8 November 2018

ABSTRACT

In cosmological N-body simulations, the baryon effects on the cold dark matter (CDM) halos can be used to solve the small scale problems in Λ CDM cosmology, such as cusp-core problem and missing satellites problem. It turns out that the resultant total density profiles (baryons plus CDM), for halos with mass ranges from dwarf galaxies to galaxy clusters, can match the observations of the rotation curves better than NFW profile. In our previous work, however, we found that such density profiles fail to match the most recent strong gravitational lensing observations. In this paper, we do the converse: we fit the most recent strong lensing observations with the predicted lensing probabilities based on the so-called (α, β, γ) double power-law profile, and use the best-fit parameters ($\alpha = 3.04, \beta = 1.39, \gamma = 1.88$) to calculate the rotation curves. We find that, at outer parts for a typical galaxy, the rotation curve calculated with our fitted density profile is much lower than observations and those based on simulations, including the NFW profile. This again verifies and strengthens the conclusions in our previous works: in Λ CDM paradigm, it is difficult to reconcile the contradictions between the observations for rotation curves and strong gravitational lensing.

Key words: gravitational lensing: strong—galaxies: haloes—cosmology: theory—dark matter.

1 INTRODUCTION

Most people believe that we are now entering a period of precise cosmology: an inflation follows immediately after the big bang, and about 13.7 billion years later, we are living in a flat universe suffused with cosmological constant (Λ) and cosmic webs made up of cold dark matter (CDM) particles and baryons. In short, we have a standard Λ CDM cosmology. There is a wide range of observational successes supporting this Λ CDM scenario, from cosmic microwave background (CMB) to the Lyman- α forest, to galaxy clustering and to weak gravitational lensing. However, three of the key ingredients remains mystery: Λ , CDM, and the scalar field that drives inflation. There are no independent experimental evidences or strong theoretical justifications for them. Clearly, they are introduced so that the previously mentioned observational successes can be achieved based on general relativity.

If we set the mystery aspects of Λ CDM cosmology aside, and enjoy our hard-won successes mainly on large scales, we still encounter some difficulties concerned with dark matter (DM) on small scales. After the universe enters matter-dominated era and nonlinear perturbations begin, the cur-

rent computer simulations become the most robust tool to explore the formation and evolution of the large scale structure (Frenk & White 2012). In the standard, hierarchical, CDM paradigm of cosmological structure formation, galaxy formation begins with the gravitational collapse of over dense regions into bound, virialized halos of CDM. In this Λ CDM paradigm, halos form from purely collisionless CDM particles with primordial power spectrum of fluctuations predicted by inflationary model. Small halos are the first to form, and larger halos form subsequently by mergers of pre-existing halos and by accretion of diffuse dark matter that has never been part of a halo. While such purely CDM N-body simulations can reproduce the observed cosmic web as demonstrated by Sloan Digital Sky Survey (SDSS), two tensions with observations arise on small scales. First, simulations show that CDM collapse leads to cuspy halos whose central density profiles have the form $r^{-\gamma}$ with $\gamma \sim 1 - 1.5$, whereas observed galaxy rotation curves suggest constant density cores with $\gamma \sim 0$. This conflict is referred as “cusp-core problem”. Second, simulations predict a large amount of subhalos formed by earlier collapses on smaller scales, but astronomers have observed much less number of satellite galaxies, which is known as the “missing satellite problem”. Recent simulations strongly suggest some connections

* E-mail: wl010@bao.ac.cn

between the two problems, or even that the two problems have merged into one (Weinberg et al. 2015).

A main type of solutions to the small scale problems is including baryons as “astrophysical processes” in originally collisionless CDM N-body simulations. This is natural in Λ CDM cosmology. On one hand, if we replace CDM with warm dark matter, the small scale problems can be resolved even without considering the influence of baryons (e.g., Shao et al. 2012). However, this is not Λ CDM cosmology anymore. On the other hand, the direct observable parts of any bound systems are made up of baryons rather than DM, so simulations must include baryons if we want to reproduce the disk galaxies and elliptical galaxies appear in our telescopes. In fact, in a simplified picture (White & Rees 1978), baryonic gas is initially well mixed with the DM particles, then participates in the gravitational collapse of DM and is heated by shocks to the virial temperature of the DM halos. Bound in the potential wells of DM halos, baryonic gas proceed to cool radiatively due to bremsstrahlung, recombination and collisionally excited line emission (Frenk & White 2012). Just before gravitational collapse, angular momentum is transferred to the aspherical perturbations by gravitational torques exerted by neighboring clumps. This results in the formation of a gas disk, and once the disk has become centrifugally supported, stars can be formed. Furthermore, the spheroidal components of disk galaxies and elliptical galaxies form by major mergers or strong gravitational encounters of disk galaxies which can lead to the complete destructions of the pre-existing disks.

In this paper, the major concern lies in the density profiles of CDM haloes based on which we can calculate rotation curves and strong lensing probabilities. The baryons have two opposite effects on the central mass density of DM halos. While stellar feedback and dynamical friction can induce expansion of the DM halo and produce a core (e.g., Shapiro, Iliev & Raga 1999, Mashchenko, Couchman & Wadsley 2006, Mashchenko, Wadsley & Couchman 2008), the adiabatic contractions can steepen central density to the singular isothermal sphere (SIS) type (Blumenthal et al. 1986; Gnedin et al. 2004; Gustafsson, Fairbairn & Sommer-Larsen 2006). Unfortunately, on one hand, a cored density profile would lead to an extremely low lensing rate compared with observations (Chen 2005; Li & Chen 2009; Chen & McGaugh 2010); on the other hand, when SIS profile matches the observations of strong lensing by giant elliptical galaxies, it fails in fitting the inner parts of rotation curves which indicate central cores. The tension between the observations of rotation curves (Katz et al. 2016; Schaller et al. 2015) and strong lensing remains for most recent high-resolution baryon+CDM simulations (Wang et al. 2017, hereafter, paper I). One such simulations (Di Cintio et al. 2014, DC14) introduce a mass-dependent density profile to describe the distribution of dark matter within galaxies, which takes into account the stellar-to-halo mass ratio (M_*/M_{halo}) dependence of baryon effects on DM. Comparing with previous similar works, a real progress for DC14 model is that it gives a density profile with inner slope depending on halo mass. At low mass end, each halo display a central core, and for halos with increasing mass, some astrophysical processes erase the central cores and steepen the inner

slopes of the DM density profiles. Since the observations of rotation curves usually come from low mass halos (such as dwarf galaxies, low surface brightness galaxies), whereas strong lensing phenomena is dominated by giant ellipticals (hosted in high mass halos), one hopes that DC14 model may resolve the tension. This can happen if the inner slope γ approaches 2 (SIS like) for halos that host giant ellipticals, which is required by strong lensing observations. However, the inner slope of DC14 model increases with halo mass only up to $\gamma \sim 1$ (NFW like) when halo mass reaches the high mass end ($\sim 10^{12}M_{\odot}$). Furthermore, the extrapolation of DC14 profile to halos with mass $> 10^{12}M_{\odot}$ exhibits no monotonic increasing of inner slope, instead, it drops dramatically after that mass (Wang et al. 2017). It thus comes as no surprise that the DC14 model generates the lensing probabilities that are much lower than both NFW and SIS models. Despite the failure for DC14 model to resolve the tension between rotation curves and strong lensing, it indeed reduces the tension. Recall that, before DC14, similar simulations give the cored density profiles which are independent of halo mass. Consequently, DC14 produces obviously higher lensing rates than cored isothermal sphere model (Wang et al. 2017). Therefore, DC14 stands for a right direction for simulations which may finally resolve the tension.

Another important example is the investigation for the internal structure and density profiles of halos of mass $10^{10} - 10^{14}M_{\odot}$ in the Evolution and Assembly of Galaxies and their Environment (EAGLE) simulations (Schaller et al. 2015, Schaller15). In this mass range the total density profile is similar to NFW in the inner and outer parts, but has a slope of -2 at some radius $r_i \sim 2.27\text{kpc}$, near the centers of halos. Schaller15 profile has no core, however, the rotation curves are in excellent agreement with observational data (Reyes et al. 2011). In paper I, we found that Schaller15 profile predicts too many lensing probabilities compared with the observations of the Sloan Digital Sky Survey Quasar Lens Search (SQLS12, Inada et al. 2012). This can be explained by the fact that, for Schaller15 halos, the central regions of halos with mass $\gtrsim 10^{12}M_{\odot}$ are dominated by the stellar component (Schaller et al. 2015). The presence of these baryons causes a contraction of the halos and thus enhances the density of DM in this regions. The over predictions of lensing probabilities for Schaller15 profile also means a failure to resolve the tension between rotation curves and strong lensing.

It is now well established that, whatever the manners the baryon effects are included in the collisionless CDM N-body cosmological simulations, if the resultant density profiles can match the observations of rotation curves, they cannot simultaneously predict the observations of strong gravitational lensing (under- or over-predict). And for the case of typical galaxies, the reverse is also true, namely, the SIS profile preferred by strong lensing cannot be supported by the observations of rotation curves near the centers of galaxies. It is unclear whether or not the reverse is true for extremely large galaxies and clusters of galaxies, which are expected to have generated the large image separations in the most recent strong lensing sample SQLS12. It is well known that, before the release of SQLS12, the SIS+NFW is a standard model to describe the well-defined statistical sample for strong lensing observational data. However, we found that

this standard model fails in describing SMLS12 (see paper I). According to the standard model, SIS and NFW profiles are used to describe the giant elliptical galaxies and clusters of galaxies respectively, the transition in mass from galaxies to clusters occurs at $M_{\text{halo}} \sim 10^{13} M_{\odot}$. We have noticed in our calculations that, simply shifting the transition mass from $M_{\text{halo}} \sim 10^{13} M_{\odot}$ to, e.g., $10^{13.5} M_{\odot}$ cannot improve the matches. Thus the failure for standard model to describe the new sample SMLS12 may imply the failure for NFW to be an appropriate model for clusters of galaxies adopted to predict lensing probabilities (Giocoli et al. 2016). If this is the case, however, we have a paradox. We know that every statistical sample consists of individual lensing systems, each of which is investigated and identified separately. Among them, each individual cluster of galaxies is always modeled by NFW profile or triaxial form of NFW, and if needed, some substructures can be added only as perturbations. So, is it reasonable that the individuals can largely be modeled as NFW but their statistical sample as a whole cannot?

Now that the results of current simulations, such as DC14 and Schaller15 profiles, are in good agreement with the observations of rotation curves but failure in predicting the strong lensing observations of SMLS12, it would be interesting to examine the converse: what a density profile, if exists, that matches the observations of SMLS12 predicts for rotation curves? To this end, in this paper, we further investigate the tension between the observations of rotation curves and strong lensing as follows. We first fit the predicted lensing probabilities based on the so-called (α, β, γ) double power-law profile directly to the SMLS12 sample, and then use the best-fit parameters (α, β, γ) for the profile to calculate rotation curves. This method can circumvent the paradox, in the sense that we just employ the well-defined sample to derive an empirical formula for the density profile, regardless of the density profile models used for each individual lensing system of the sample.

This paper is organized as follows: in Section 2 we fit (α, β, γ) double power-law model to the most recent strong lensing sample SMLS12 to obtain a density profile of DM haloes. In Section 3, the rotation curves calculated based on the fitted density profile are compared with observations and other models. The discussions and conclusions are presented in Section 4.

2 FITTING THE DENSITY PROFILE

The predicted lensing probabilities are determined by the assumed density profile of lensing objects. Therefore, in order to obtain an empirical formula for a density profile from strong lensing sample, one should first assume a functional form of the density profile with some free parameters; then fit the predicted lensing probabilities (based on the assumed density profile) to that of SMLS12 sample to get the values of the parameters.

We employ the so-called (α, β, γ) double power-law model as the assumed density profile for lenses

$$\rho(r) = \frac{\rho_s}{\left(\frac{r}{r_s}\right)^\gamma \left[1 + \left(\frac{r}{r_s}\right)^\alpha\right]^{(\beta-\gamma)/\alpha}}, \quad (1)$$

where ρ_s is the scale density and r_s the scale radius. In this

paper, we treat (α, β, γ) as free constant parameters to be determined from the fitting, in contrast to DC14 model, in which they are halo mass dependent.

The corresponding surface mass density is

$$\Sigma(x) = 2\rho_s r_s V(x) \quad (2)$$

where

$$V(x) = \int_0^\infty (x^2 + z^2)^{-\gamma/2} \left[(x^2 + z^2)^{\alpha/2} + 1 \right]^{(\gamma-\beta)/\alpha} dz,$$

and $x = |\vec{x}|$, $\vec{x} = \vec{\xi}/r_s$, $\vec{\xi}$ is the position vector in the lens plane. We thus obtain the lensing equation

$$y = x - \mu_s \frac{g(x)}{x}, \quad (3)$$

where $y = |\vec{y}|$, $\vec{\eta} = \vec{y} r_s D_S / D_L$ is the position vector in the source plane, and

$$g(x) \equiv \int_0^x u V(u) du, \quad (4)$$

and

$$\mu_s \equiv \frac{4\rho_s r_s}{\Sigma_{\text{cr}}}, \quad (5)$$

where $\Sigma_{\text{cr}} = (c^2/4\pi G)(D_S/D_L D_{\text{LS}})$ is the critical surface mass density; D_L , D_S and D_{LS} are the angular diameter distances from the observer to the lens, to the source and from the lens to the source, respectively.

When the quasars of redshift z_s are lensed by foreground CDM halos of galaxy clusters and galaxies, the lensing probability with image separations larger than $\Delta\theta$ is (Schneider et al. 1992)

$$P(> \Delta\theta) = \int_0^{z_s} \frac{dD_L^{\text{P}}(z)}{dz} dz \times \int_0^\infty \bar{n}(M, z) \sigma(M, z) B(M, z) dM, \quad (6)$$

where $D_L^{\text{P}}(z)$ is the proper distance from the observer to the lens located at redshift z . We make $z_s = 1.56$ for statistical sample SMLS (Inada et al. 2012). The physical number density $\bar{n}(M, z)$ of virialized DM halos of masses between M and $M + dM$ is related to the comoving number density $n(M, z)$ by $\bar{n}(M, z) = n(M, z)(1+z)^3$. As in paper I, $n(M, z)$ was originally given by Press & Schechter (1974), and we use the improved version given by Sheth & Tormen (1999). The cross-section is $\sigma(M, z) = \pi y_{\text{cr}}^2 r_s^2 \vartheta(M - M_{\text{min}})$, where y_{cr} is the maximum value of y , the reduced position of a source, such that when $y < y_{\text{cr}}$ multiple images can occur; $\vartheta(x)$ is a step function, and M_{min} is the minimum value of the halo mass that can produce image separation $\Delta\theta$. Also, as in paper I, for the magnification bias $B(M, z)$, we adopt a simple model (Li & Ostriker 2002): $B \approx 2.2 A_m^{1.1}$, with $A_m = D_L \Delta\theta / (r_s y_{\text{cr}})$.

Cleanly, the free parameters (α, β, γ) have entered into $P(> \Delta\theta)$ via equations (1), (2) and cross-section σ , together with magnification bias B , whence we get the corresponding predicted number counts of lenses with image separations larger than $\Delta\theta$ for the sample SMLS12 as

$$n(> \Delta\theta; \alpha, \beta, \gamma) = NP(> \Delta\theta), \quad (7)$$

where $N = 50836$ is the number of source quasars

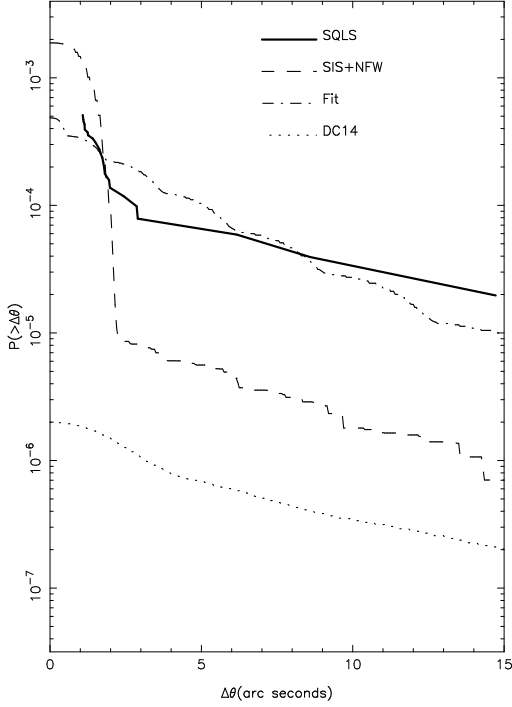


Figure 1. Lensing probabilities with image separations larger than $\Delta\theta$: observations for SMLS sample (thick histogram), and the predictions for the models of SIS +NFW (dashed line), our fitting result (dot-dashed line) and DC14 (dotted line).

from which 26 lenses are selected for the sample SMLS12 (Inada et al. 2012).

We use least-square fit method. Choose a merit function that measures the agreement between the data and the model with a particular choice of parameters. The merit function is conventionally arranged so that small values represent close agreement. The parameters of the model are then adjusted to achieve a minimum in the merit function, yielding best-fit parameters. The adjustment process is thus a problem in minimization in many dimensions. At last we get the best-fit parameters: $\alpha=3.04$, $\beta=1.39$ and $\gamma=1.88$.

The predicted lensing probability for our fitting model (dot-dashed line) is displayed in Fig.1, together with the observations of SMLS12 sample (thick histogram), the predictions for the models of SIS+NFW (dashed line) and DC14 (dotted line). The latter two lines are copied from paper I.

It turns out that our fitted one-population (α, β, γ) double power-law model can only roughly predict the strong lensing observations of SMLS12. Hence some two-population models, like SIS+NFW, are still preferred by better fittings. However, it suffices for the aim of this paper: We just need a density profile alternative to DC14 and Schaller15 models that can predict lensing observations of SMLS12 much better than the latter, which are also of one-population.

Before investigating the rotation curves, it is helpful for us to compare some properties of the fitted density profile with other models, such as NFW, DC14 and Schaller15. Note that, for a given halo mass, the density profiles for different models can be plotted only when some additional parameters have been determined. For the (α, β, γ) double power-law model, such parameters are (see paper I)

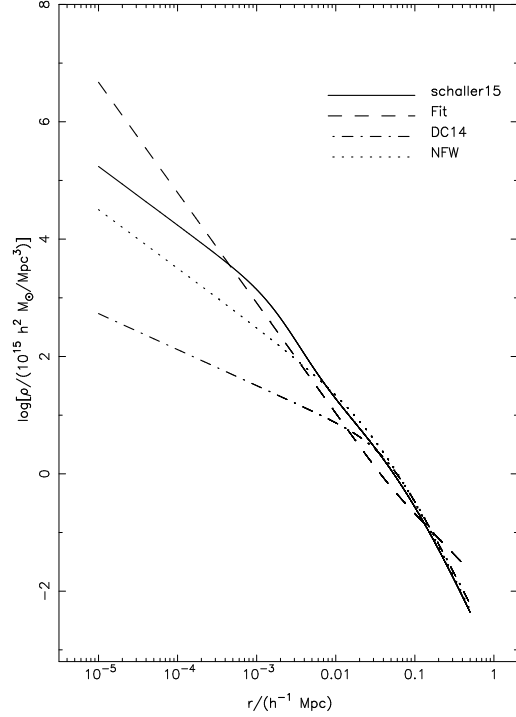


Figure 2. The density profiles for different models for a typical galaxy with halo mass $M_{\text{halo}} = 10^{13} M_{\odot}$: Schaller15 (solid line), our fit model (dashed line), DC14 (dot-dashed line) and NFW (dotted line).

$$\rho_s = \rho_{\text{crit}} \left[\Omega_m (1+z)^3 + \Omega_{\Lambda} \right] \frac{200}{3} \frac{c_1^3}{f(c_1)}, \quad (8)$$

$$r_s = \frac{1.626}{c_1} \frac{M_{15}^{1/3}}{[\Omega_m (1+z)^3 + \Omega_{\Lambda}]^{1/3}} h^{-1} \text{Mpc}. \quad (9)$$

where ρ_{crit} is the present value of the critical mass density of the universe, and M_{15} is the reduced mass of a halo defined as $M_{15} = M_{\text{halo}} / (10^{15} h^{-1} M_{\odot})$. The concentration parameter c_1 is approximately a constant and we have adopted $c_1 \simeq 9$ (but see Gao et al. 2008). And

$$f(c_1) = \int_0^{c_1} \frac{x^2 dx}{x^{\gamma} (1+x^{\alpha})^{(\beta-\gamma)/\alpha}}. \quad (10)$$

Therefore, ρ_s and r_s are redshift-dependent, we choose $z = 0.45$ for a typical lens. Clearly, DC14 and NFW models have the same functional forms of ρ_s and r_s as equations (8) and (9), they differ only in different values of (α, β, γ) . For DC14 these parameters are halo mass dependent, and for NFW, $(\alpha, \beta, \gamma) = (1, 3, 1)$. For Schaller15 profile,

$$\frac{\rho(r)}{\rho_{\text{crit}}} = \frac{\delta_c}{\left(\frac{r}{r_s}\right) \left(1 + \frac{r}{r_s}\right)^2} + \frac{\delta_i}{\left(\frac{r}{r_i}\right) \left[1 + \left(\frac{r}{r_i}\right)^2\right]}, \quad (11)$$

where the parameters δ_c , δ_i and r_s are all fitted to halo mass with the data given by Schaller et al. (2015), and $r_i = 1.7 h^{-1} \text{kpc}$ for all halo masses (see paper I).

The density profiles are presented for different models in Fig.2 and Fig.3 for the cases when a typical galaxy has halo mass of $M_{\text{halo}} = 10^{13} M_{\odot}$ and a typical cluster of galaxies has halo mass of $M_{\text{halo}} = 10^{15} M_{\odot}$, respectively. For a double

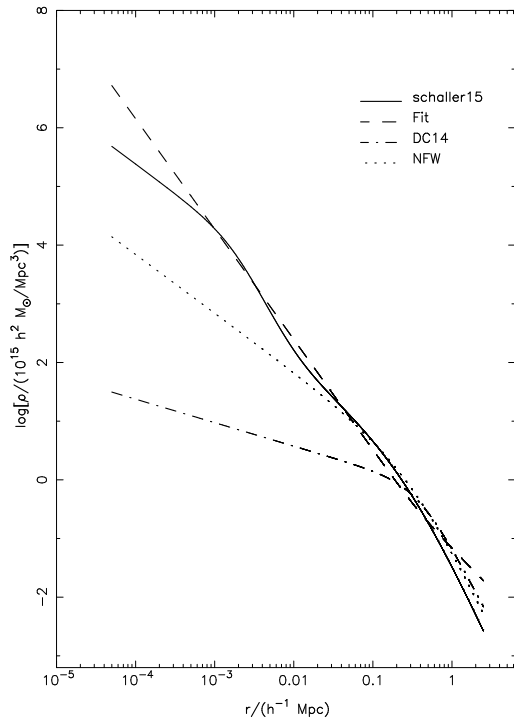


Figure 3. The density profiles for different models for a typical cluster of galaxies with halo mass $M_{\text{halo}} = 10^{15} M_{\odot}$: Schaller15 (solid line), our fit model (dashed line), DC14 (dot-dashed line) and NFW (dotted line).

power-law model, γ and β are the inner and outer slope respectively, and α describes the transition between the two.

For a typical galaxy (Fig.2), the slope of our fitted density profile ($\gamma = 1.88$) is larger than other models in the innermost regions. This value is close to SIS model ($\gamma = 2$), which is required to explain the observations for galactic halos as lenses. The slope approaches 1.39 at outer regions, which is obviously lower than SIS (~ 2) and NFW (~ 3). Notice that, for Schaller15 profile, the slope has the value of 1 in the innermost regions, 2 at the radius $r = r_i = 1.7 h^{-1} \text{kpc}$ (very near the center), and approaches to 3 in the outer regions (NFW like). This can explain the over-predictions to SQLS12 for Schaller15 model in terms of slopes. As for DC14 profile, in most regions starting from the center, the slope is flatter than NFW, and it reaches 3 (NFW like) only in very outer regions. This can explain why DC14 model predict too few lenses.

For a typical cluster of galaxies (Fig.3), we find that our fitted density profile has almost the same slope as of Schaller15 in the regions between $r_i \sim \text{kpc}$ and $\sim 500 \text{kpc}$, whereas it is steeper than Schaller15 in the innermost regions ($< r_i$), and flatter in outer regions ($\gtrsim 500 \text{kpc}$). Therefore, the overpredictions of Schaller15 model (Fig.1) suggest that the profiles with flatter outer slopes (flatter than NFW) are preferred.

3 ROTATION CURVES

The observations of rotation curves provide us independent evidences for or against a density profile model. While sim-

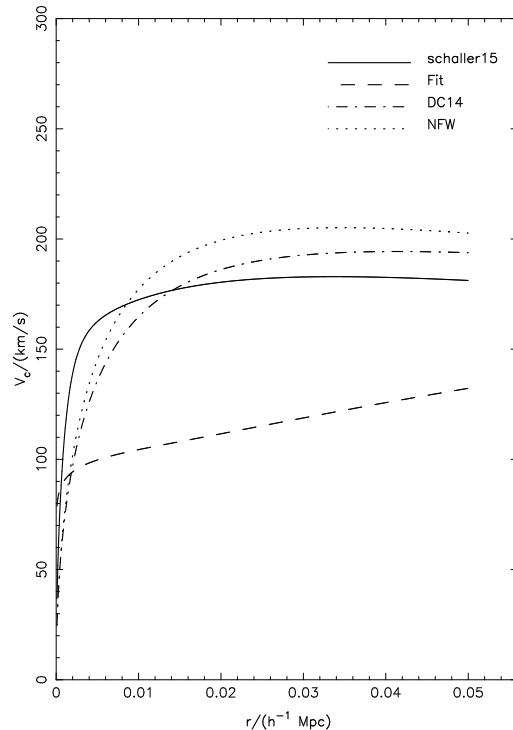


Figure 4. Rotation curves for different models: Schaller15 (solid line), our fit model (dashed line), DC14 (dot-dashed line) and NFW (dotted line).

ulations suggest some density profiles that are in agreement with the observations of rotation curves, e.g., Schaller15, we find that they cannot predict the most recent observations of strong gravitational lensing. It is thus very interesting to investigate the behavior of rotation curves for the density profile fitted from the observations of strong lensing in previous section. For a given spherically symmetric density profile $\rho(r)$, the Poisson's equation

$$\frac{1}{r^2} \frac{\partial}{\partial r} \left(r^2 \frac{\partial \Phi}{\partial r} \right) = 4\pi G \rho \quad (12)$$

leads to the circular velocity

$$V_c^2 = r \frac{d\phi}{dr} = \frac{4\pi G}{r} \int_0^r \rho(r') r'^2 dr', \quad (13)$$

where we have required $\lim_{r \rightarrow 0} V(r) \rightarrow 0$.

Assuming a typical disk galaxy with halo mass $\sim 10^{12} M_{\odot}$, the rotation curves predicted by different density profiles can be obtained by numerical integrating via equation (13). The results are displayed in Fig.4 for the density profiles of our fit model (dashed), Schaller15 (solid), DC14 (dot-dashed) and NFW (dotted), respectively. It can be easily recognized that, in the flat part, the rotation curve of our fit model is much lower than that of other three models, which are around 200km/s , a typical observed value for a halo with mass of $\sim 10^{12} M_{\odot}$. Therefore, our fitted density profile from strong lensing observations is ruled out by the observations of rotation curves.

We have repeatedly emphasized that strong lensing is very sensitive to the inner slopes of the assumed density profiles of lensing halos (Chen 2005; Li & Chen 2009; Chen & McGaugh 2010), however, this is true only when

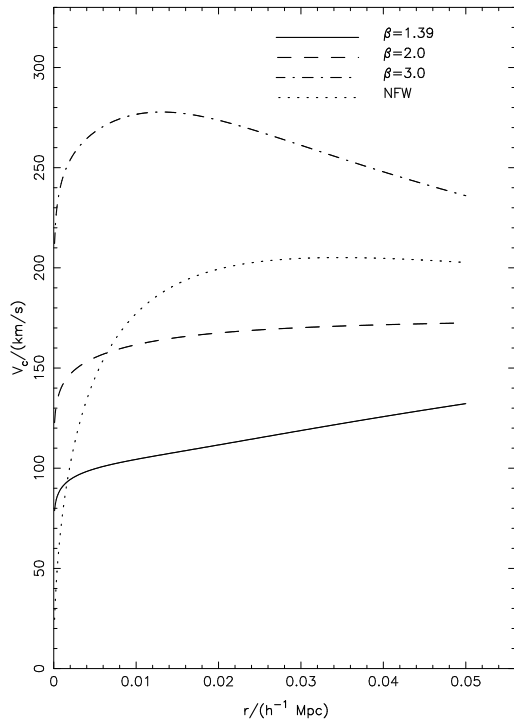


Figure 5. The rotation curves for NFW model (dotted line), our fit model $(\alpha, \beta, \gamma) = (3.04, 1.39, 1.88)$ (solid line), and the cases when $(\alpha, \beta, \gamma) = (3.04, 2.0, 1.88)$ (dashed line) and $(\alpha, \beta, \gamma) = (3.04, 3.0, 1.88)$ (dot-dashed line).

the concentration parameters ($c = r_{200}/r_s$ for NFW and the like, CP hereafter) for different models are fixed in actual lensing probability calculations (Sarbu, Rusin, & Ma 2001; Li & Ostriker 2002; Chen 2003a,b, 2004a,b; Zhang 2004). We know that CP reflects a slope distribution starting from the innermost region out to the outer regions of a halo. Hence if CP is treated as a changeable parameter, it would be more important than the inner slope to lensing efficiency (Giocoli et al. 2012). On the other hand, just like strong lensing efficiencies, different rotation curves are predicted by different total (DM+baryon) density profiles of galactic halos, and hence are also very sensitive to the concentration parameter c (McGaugh 2016). Therefore, both lensing efficiencies and rotation curves are sensitive not only to inner slopes but also to outer slopes. For strong lensing, the outer slope of our fitted profile ($\beta \sim 1.39$) is smaller than Schaller15 profile (~ 3), which results in the overpredictions of the latter to the observations of SQLS12 (Fig.1). For rotation curves, this can be easily verified by changing outer slopes. To see this, in Fig.5, we present the rotation curves that are predicted based on our fit model (solid line), and the models by keeping $\alpha = 3.04$ and $\gamma = 1.88$ unchanged, while increasing outer slope β to 2 (SIS like, dashed line) and 3 (NFW like, dot-dashed line). Clearly, the outer parts of rotation curves increase with increasing outer slope.

4 DISCUSSIONS AND CONCLUSIONS

We have used the (α, β, γ) double power-law model to fit the most recent strong lensing observations SQLS12, and get

the best-fit parameters $\alpha=3.04$, $\beta=1.39$ and $\gamma=1.88$. It turns out that the outer part of the rotation curve predicted by this fitted density profile is much lower than that predicted by other models which can account for the observations. So we conclude that the density profile of DM haloes that can predict the most recent observations of strong lensing cannot predict the observations of rotation curves.

In a certain sense, we admit that, the one-population, (α, β, γ) double power-law model is a toy model when applied to strong lensing sample SQLS12 which include both galaxies and clusters of galaxies. In strong lensing statistics, we usually employ a two-population SIS+NFW model. However, as is pointed out earlier, in this two-population model, NFW is not enough to account for the lensing rates of large image separations. What’s more, we indeed have a “universal” density profile, NFW, which still serves us as starting point in current N-body cosmological simulations. Including baryon effects can only change the slopes near the centers of haloes. In particular, Schaller15 model is only the most recent example of the similar simulations which are of one-population and are valid both for galaxies and clusters (Shapiro, Iliev & Raga 1999; Mashchenko, Couchman & Wadsley 2006; Mashchenko, Wadsley & Couchman 2008). Of course, it seems impossible that, in simulations, the baryon effects can reproduce such shallow outer slopes as $\beta \sim 1.4$ of our fit model. The problem is, even if some mechanisms in simulations can do the job, this shallow outer slope is incompatible with the observations of rotation curves.

At first sight, it is a temptation to fit the lensing sample with (α, β, γ) double power-law model but allow α, β , and γ all to be halo mass-dependent, as done by Di Cintio et al. (2014) when they fit their simulations. Unfortunately, more than a dozen of free parameters involved and the high degeneracy between lensing probabilities and density profiles make it impossible for merit functions to be convergent.

On the other hand, we may consider some two-population fittings. As is well-known, SIS has been proved to be a good model to account for giant ellipticals as lenses. But SIS is in conflict with the observations of rotation curves which indicates a constant core for most disk galaxies (de Blok et al. 2001, 2008; de Blok 2010; McGaugh et al. 2007). As for clusters of galaxies, they have nothing to do with rotation curves. So two-population fittings cannot do better than one-population (α, β, γ) double power-law model on the subject in this paper.

As a summary, in paper I and other previous works, we find that the density profiles of DM haloes which are in agreement with observations of rotation curves cannot match the observations of strong lensing probabilities; in this paper, we find that the converse is also true, namely, the density profiles fitted from strong lensing probabilities cannot predict the observations of rotation curves. So we conclude that, in Λ CDM paradigm, it is difficult to reconcile the contradictions between the observations of rotation curves and strong gravitational lensing.

ACKNOWLEDGEMENTS

This work was supported by the National Natural Science Foundation of China (Grant 11073023). RL is supported by Youth Innovation Promotion Association of CAS.

REFERENCES

- Blumenthal G.R., Faber S. M., Fores R., Primack J. R., 1986, *ApJ*, 301, 27
- Chen D. -M., 2003a, *A&A*, 397, 415
- Chen D. -M., 2003b, *ApJ*, 587, L55
- Chen D. -M., 2004a, *A&A*, 418, 387
- Chen D. -M., 2004b, *Chinese J. Astron. Astrophys.*, 4, 118
- Chen D.-M., 2005, *ApJ*, 629, 23
- Chen D. -M., McGaugh S., 2010, *RAA*, 10, 1215
- Crocce M., Fosalba P., Castander F. J., Gaztanaga E., 2010, *MNRAS*, 403, 1353
- de Blok W. J. G., McGaugh S. S., Bosma A., Rubin V. C., 2001, *ApJ*, 552, L23
- de Blok W. J. G., Walter F., Brinks E., Trachternach C., Oh S.-H., Kennicutt R. C., Jr, 2008, *AJ*, 136, 2648
- de Blok W. J. G., 2010, *Advances in Astronomy*, Volume 2010, Article ID 789293
- Di Cintio A., Brook C. B., Dutton A. A., Maccio A. V., Stinson G. S., Knebe A., 2014, *MNRAS*, 441, 2986
- Frenk C. S., White S. D. M., 2012, *Annalen der Physik*, 524, 507
- Gao L., Navarro J. F. , Cole S., Frenk C. S., White S. D. M., Springel V., Jenkins A., Neto A. F., 2008, *MNRAS*, 387, 536
- Giocoli C., Meneghetti M., Bartelmann M., Moscardini L., Boldrin M., 2012, *MNRAS*, 421, 3343
- Giocoli C., Bonamigo M., Limousin M., Meneghetti M., Moscardini L., Angulo R. E., Despali G., Jullo E., 2016, *MNRAS*, 462, 167
- Gnedin O. Y., Kravtsov A. V., Klypin A. A., Nagai D., 2004, *ApJ*, 616, 16
- Gustafsson M., Fairbairn M., Sommer-Larsen J., 2006, *Phys. Rev. D*, 74, 123522
- Inada N. et al., 2012, *AJ*, 143, 119
- Katz H., Lelli F., McGaugh S. S., Di Cintio A., Brook C. B., Schombert J. M., 2017, *MNRAS*, 466, 1648
- Li L. -X., Ostriker J. P., 2002, *ApJ*, 566, 652
- Li N., Chen D.-M., 2009, *RAA*, 9, 1173
- Mashchenko S., Couchman H. M. P., Wadsley J., 2006, *Nature*, 442, 539
- Mashchenko S., Wadsley J., Couchman H. M. P., 2008, *Science*, 319, 174
- McGaugh S. S., 2016, *ApJ*, 816, 42
- McGaugh S. S., de Blok W. J. G., Schombert J. M., Kuzio de Naray R., Kim J. H., 2007, *ApJ*, 659, 149
- Press W. H., Schechter P., 1974, *ApJ*, 187, 425
- Reyes R., Mandelbaum R., Gunn J. E., Pizagno J., Lackner C. N., 2011, *MNRAS*, 417, 2347
- Sarbu N., Rusin D., Ma C. -P., 2001, *ApJ*, 561, L147
- Schaller M. et al., 2015, *MNRAS*, 451, 1247
- Schneider P., Ehlers J., Falco E. E., 1992, *Gravitational Lenses* (Berlin: Springer-Verlag)
- Shao S., Gao L., Theuns T., Frenk C. S., 2012, *MNRAS*, 430, 2346
- Shapiro P. R., Iliev I. T., Raga A. C., 1999, *MNRAS*, 307, 203
- Sheth R. K., Tormen G., 1999, *MNRAS*, 308, 119
- Wang L., Chen D.-M., Li R., 2017, *MNRAS*, preprint (arXiv: 1706.03324v1)
- Weinberg D. H., Bullock J. S., Governato F., de Naray R. K., Peter A. H. G., 2015, *Proc. Natl. Acad. Sci.*, 112, 12249
- White S. D. M., Rees M. J., 1978, *MNRAS*, 183, 341
- Zhang T. -J., 2004, *ApJ*, 602, L5